DOI: 10.21062/mft.2022.045 http://www.journalmt.com

Partial Substitution of Mn by Al in the Cocrfenimnxal20-X (X=5, 10, 15) High Entropy Alloy Prepared of Mechanical Alloying and Spark Plasma Sintering

Hana Thürlová (0000-0001-7011-5573)*, Filip Průša (0000-0002-6494-5084)
Department of Metals and Corrosion Engineering, University of Chemistry and Technology Prague. Technická 5, 166 28 Prague 6. Czech Republic. E-mail: *thurlovh@vscht.cz

High-entropy alloys are known to possed good mechanical properties which are usually related to the preparation technique. In this work, the $CoCrFeNiMn_XAl_{20-X}$ (X=5, 10, 15) alloys were prepared by a combination of mechanical alloying (MA) and compacted via spark plasma sintering (SPS). Such prepared materials were examined for their phase composition and microstructure. Furthermore, their mechanical properties as a result of the content of Mn/Al were determined. It was found, that the partial substitution of Mn by Al lead to increasing the volume content of the solid solution with BCC crystallographic lattice within the ultrafine-grained microstructure of such prepared materials. Moreover, increasing the Al content within the alloy lead also to the improvement of the mechanical properties. The CoCrFeNiMn5Al15 alloy reached the best properties of all the alloys showing compressive strength of 2496 MPa and having a hardness of 668 HV 1.

Keywords: Mechanical alloying, spark plasma sintering, high entropy alloys, mechanical properties.

1 Introduction

The high-entropy alloys belong to modern materials which are typically known for their high mixing entropy. Accordingly to the definition, they are composed usually of 5 or more elements with concentrations ranging between 5 – 35 at.% [1]. Due to the high mixing entropy, the microstructure of these materials is foremostly composed of disordered solid solutions having either FCC, BCC or HCP crystallographic lattices [1] accordingly to the majority of elements that are forming the solid solution.

These materials can be prepared by a variety of methods including powder metallurgy techniques, induction melting or additive manufacturing. The chosen preparation technique and its parameters strongly affect the mechanical properties of prepared high-entropy alloys, which are generally having highly promising properties combined, e.g. high yield strength and ultimate strength with sufficient ductility [1]. The high-entropy alloys are nowadays prepared also by non-conventional methods such as additive manufacturing, which allows for preparing semi-products with complex shapes. For this purpose, the Selective Laser Melting (SLM) method is the most used. The powder particles of the HEA are melted using a high-energy laser scanning over the surface of the material [2]. The main disadvantage of this process is the porosity of such prepared materials which strongly deteriorates the resulting material properties [3]. Thus, the most promising technique up to these days for the preparation of HEAs with outstanding properties is powder metallurgy. The HEAs which were prepared by the combination of mechanical alloying (MA) and compacted via spark plasma sintering (SPS) [4] are known to retain certain internal stress-strains while the compaction method is known to significantly lower porosity even on the level of the internal porosity present within the powder particle interior. This porosity reduction is related to the compaction temperature which is typically for SPS lower compared to other compaction techniques [5]. Another advantage of powder metallurgy is the ability to prepare ultrafine-grained materials [4, 6, 7]. Thanks to this, the alloys prepared by mechanical alloying are showing significantly higher strengths and hardnesses compared to identical alloys prepared by more conventional techniques, e.g. induction melting and casting [1, 7, 8].

The CoCrFeNiMN alloy belongs to the most pronounced HEAs, well known for their beneficial combination of mechanical properties, which can be modified in a wide range accordingly to chosen preparation method. If it is prepared by powder metallurgy techniques, it may achieve the highest hardness of 352 HV 30 and ultimate compressive strength (UCS) of 1610 MPa [1, 9]. Additionally, being composed of a solid solution with FCC crystallographic lattice is responsible for having good ductility [9]. Another example of the HEAs prepared by the identical process is CoCrFeNiAl alloy which is having solid solution with BCC lattice [10]. Therefore, the mechanical properties of this alloy are even better compared to the CoCrFeNiMn having a hardness of 625 HV 30 and UCS of 1907 MPa [10]. On the other hand, the increase in hardness and strength is balanced by a decrease in ductility of such alloy. Therefore, this work aimed to determine the influence of partial substitution of Mn by Al in the CoCrFeNiMnAl to maximize the mechanical properties, namely the strength while maintaining sufficient ductility.

2 Experimental

The powder CoCrFeNiMn15Al5, CoCrFeNiMn10Al10 and CoCrFeNiMn5Al15 alloys were prepared by MA in the planetary ball milling device Retsch PM 100 in the Ar atmosphere. The milling jar as well as the milling balls, which weight ratio to the alloyed powder was 15:1, were made of stainless steel AISI 420. A 4 wt.% of n-heptane were added to the alloyed powder to minimize the deleterious cold welding of the powder to the jar and balls. MA was done using a rotational speed of 400 rpm with an 8h of total process time where a 10 min break each 30 min of the process was implemented.

Prepared powder alloys were further processed by an SPS compaction. This step included a 10g powder batch placed into the graphite die (see Fig. 1) and heating it with a speed of 200 °C/min until reaching the compaction temperature of 1000 °C. The sample was then compacted using a pressure of 48 MPa within 1 min and remained compressed at this temperature for another 9 min after which cooling was with maximal speed. The prepared powders as well as compact samples were further investigated for their chemical (XRF) and phase (XRD) compositions. The metallographic cross-sections were ground on SiC abrasive papers P400-P2500 and polished on polycrystalline suspensions with particle sizes of 3 and 1 μm. The microstructure of the etched samples (aqua regia composed of HNO_3 and HCl mixed in a ratio of 3:1 further diluted in a ratio of 1:1 with distilled H_2O) was observed using the light microscope Nikon Eclipse MA 200. Detailed observation of the microstructure was done using the scanning electron microscope SEM TESCAN LYRA 3.

The mechanical properties of compact samples were described by the Vickers hardness measurements (1 kg load, 10 s dwell time) using the Future-Tech FM-700 device accordingly to ČSN EN ISO 6507-1. For each of the studied materials, at least 10 measurements were done and their results are expressed as average values with a confidence interval at the significance level $\alpha = 0{,}05$. Furthermore, compressive stress-strain tests were done on cubical-like samples having a strain speed of 0.001 s-1 accordingly to the DIN 50 106. Average values of compressive yield strength and ultimate compressive strength were calculated using at least values from three individual tests of each sample.

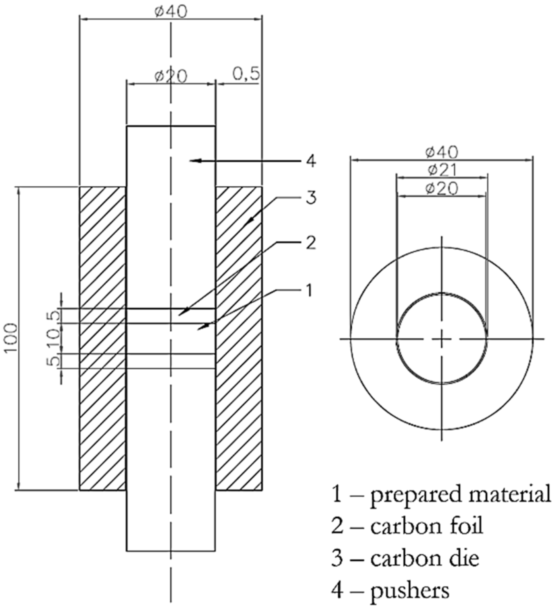

Fig. 1 *Scheme of the graphite form assembly used for powders compaction via SPS*

3 Results and discussion

3.1 Chemical and phase composition

The chemical composition of the MA+SPS alloys was determined by the XRF analysis (Tab. 1). Accordingly, to that results, the alloys were nearly having the intended compositions. The minor deviations in the compositions were caused by the different behaviour of each element during the initial steps of MA, where some of the powders tend to immediately stick to the walls of the milling jar/elements. In addition, we also observed an increasing content of Fe originating from the milling jar within the alloy which corresponded to the formation of the solid solution manifesting itself with a steep increase in the hardness. The presence of Si in all of the prepared materials reaching up to 2.3 at.% was caused due to mechanical cleaning of the milling jar using SiC abrasive powders, which tend to get stuck into the alloying equipment.

Tab. 1 *Chemical composition of the MA+SPS alloys*

alloy	concentration [at.%]						
	Co	Cr	Fe	Ni	Mn	Al	Si
CoCrFeNiMn15Al5	15.6	18.0	21.1	24.9	14.8	4.1	1.5
CoCrFeNiMn10Al10	18.6	19.4	21.8	20.7	9.3	8.5	1.7
CoCrFeNiMn5Al15	18.4	18.6	23.0	20.8	4.4	12.5	2.3

Based on the XRD analysis results (Tab. 2), the higher the Al content, the lower the volume fraction of FCC solid solution. On the other hand, the content of the BCC solid solution did not change throughout the alloys except the CoCrFeNiMn5Al15. The FCC solid solution content was decreased at the expense of the newly formed phase with primitive cubic (PC) lattice, which was identified as AlNi (JCPDS card no. 01-073-2594). Except for the mentioned phases, a formation of carbides during the SPS compaction was observed as a result of the reaction with the carbon mould. The volume fraction of such formed carbides was really low and therefore was not accounted into the phase composition balance.

Tab. 2 *Phase composition of MA+SPS alloys*

alloy	concentration [%]		
	FCC	BCC	PC
CoCrFeNiMn15Al5	63	34	3
CoCrFeNiMn10Al10	50	34	16
CoCrFeNiMn5Al15	36	25	39

3.2 Microstructure

The microstructure of powder alloys was observed by the means of LM to determine the internal porosity present within the powder particle‘s interior. The porosity was determined by the threshold method in the ImageJ software using the micrographs of non-etched samples (see Tab. 3). The average surface porosity of all the materials was below 2% and decreased with increasing content of Mn reaching its minima in the case of CoCrFeNiMn15Al5 alloy.

Tab. 3 *Average surface porosity of the prepared powder alloys*

alloy	porosity [%]
CoCrFeNiMn15Al5	1.18 ± 0.21
CoCrFeNiMn10Al10	1.37 ± 0.13
CoCrFeNiMn5Al15	1.97 ± 0.25

The LM micrographs of the prepared powder alloys show a presence of ultrafine-grained microstructure with some internal porosity manifesting themselves as black spots within the powder particle‘s interior (see Fig. 2). The microstructure did not undergo any significant change as the content of Mn/Al changed showing the presence of some areas with a regularly alternating ductile FCC and hard but brittle BCC and PC phases. Due to the MA, the phases' diameter was significantly refined down to the sub-micrometre range and the microstructure was showing traces of their intermixing.

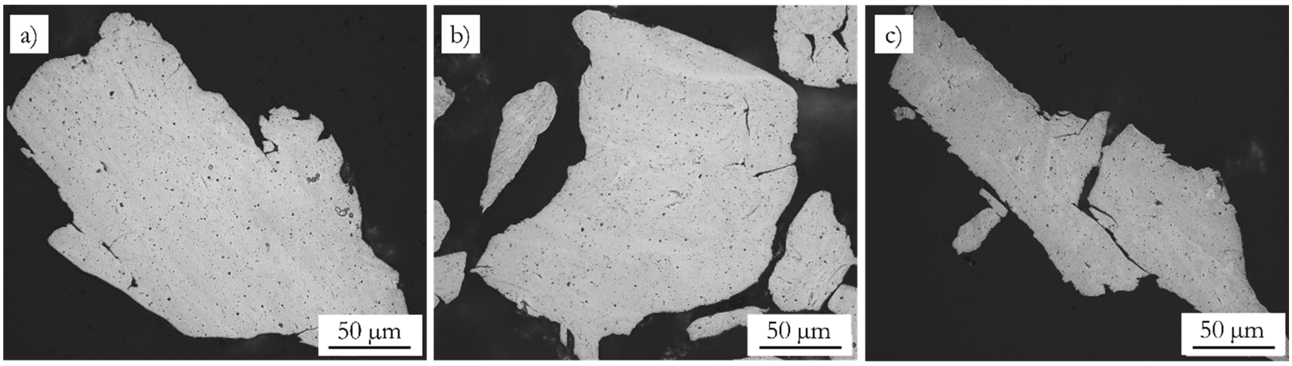

Fig. 2 *Microstructure of the 8h MA powders of: a) CoCrFeNiMn15Al5; b) CoCrFeNiMn10Al10; c) CoCrFeNiMn5Al15 alloys*

After the SPS compaction, a surface porosity reduction was observed in all of the prepared alloys. Newly, the compacts showed surface porosity that did not exceed 1.5% (see Tab. 4). The main reason for the porosity reduction was the significant plastic deformation during the SPS compaction at an elevated temperature of 1000 °C. This allowed reducing the internal porosity that was observed in the case of the aforementioned powder particles.

Tab. 4 *Relative porosity of compacted alloys*

alloy	porosity [%]
CoCrFeNiMn15Al5	1.41 ± 0.19
CoCrFeNiMn10Al10	0.97 ± 0.14
CoCrFeNiMn5Al15	1.06 ± 0.08

The microstructure appearance changed during the SPS compaction showing the absence of lamellar structure formerly observed in the case of prepared powders. Moreover, it retained its beneficial ultrafine-grained morphology as is shown in Fig. 3. The submicrometre present phases were homogeneously dispersed which is characteristic of the HEAs. In addition, the porosity of these compacts was showing significantly lower content of nano-sized pores at the expense of macro-pores, which were located at the contact points of the individual particles.

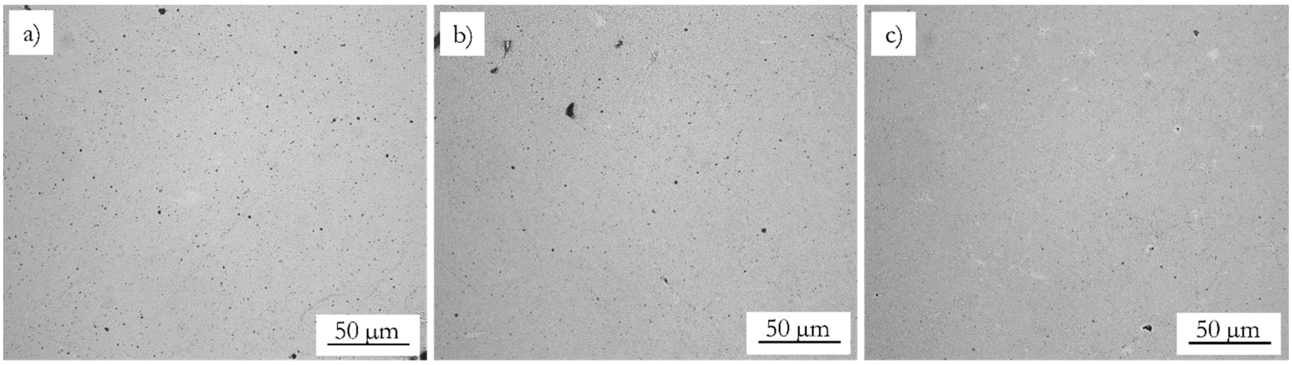

***Fig. 3** Microstructure of compact: a) CoCrFeNiMn15Al5; b) CoCrFeNiMn10Al10; c) CoCrFeNiMn5Al15 alloys*

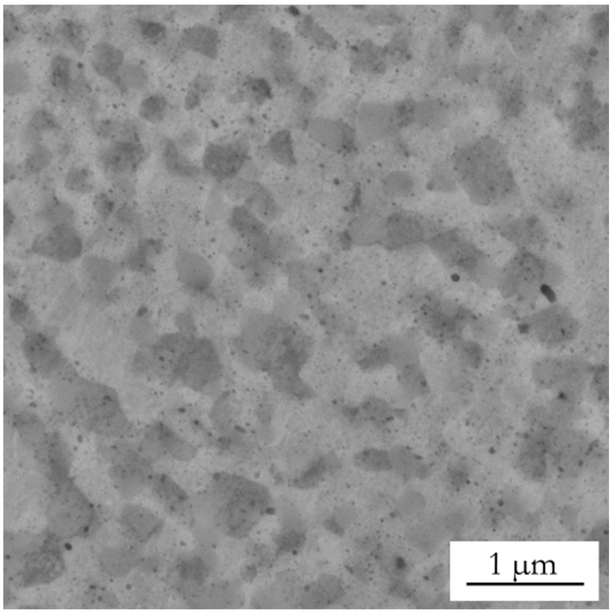

***Fig. 4** Microstructure of CoCrFeNiMn10Al10 alloy (MA+SPS)*

The more detailed SEM micrograph of the CoCrFeNiMn10Al10 alloy (Fig. 4) shows foremostly the presence of FCC and BCC solid solutions and a small amount of the PC phase. For this purpose, the micrograph was taken using a back-scatter electron detector which allows displaying chemical contrast within the material. Therefore, the medium grey areas corresponded to the presence of FCC solid solution (depleted of Al), while the dark-grey areas were identified as grains of BCC solid solution (enriched of Al) and the light-grey areas corresponded to the presence of PC phase. The microstructure of the CoCrFeNiMn15Al5 a CoCrFeNiMn5Al15 was showing similar microstructural features, although their proportions were slightly different (see Tab. 2).

The SEM micrographs of the etched compacts were used to determine the grain sizes using Feret‘s diameter measurements (Tab. 5). Accordingly, to hereby stated results, the grain size of the BCC phase (the most distinguishable ones) ranged from 263 up to 293 nm confirming the ultrafine-grained character of the compact samples. Moreover, it was shown that the actual chemical composition did not affect the grain sizes which were, considering the standard deviation, almost identical.

***Tab. 5** Grain size of prepared alloys*

alloy	grain size [nm]
CoCrFeNiMn15Al5	263 ± 58
CoCrFeNiMn10Al10	293 ± 71
CoCrFeNiMn5Al15	292 ± 64

3.3 Mechanical properties

The mechanical properties of the prepared compact samples were evaluated by the Vickers hardness measurements and by the compressive stress-strain tests at laboratory temperature, which results are shown in Tab 5. Regarding the hardness, the highest value was measured in the case of CoCrFeNiMn5Al15 alloy, which was also characterized by the lowest volume fraction of the FCC solid solution. The same behaviour could be observed during the compressive stress-strain tests where the increasing content of Al increases especially the compressive yield strength while the ultimate compressive strength showed only a minor increase of 160 MPa in total. It can be seen that the best properties among all the alloys were achieved in the case of the aforementioned CoCrFeNiMn5Al15 alloy having CYS of 2135 ± 21 MPa and UCS of 2496± 21 MPa, respectively. However, the highest mechanical properties were achieved at the expense of reduced ductility reaching only 15 %. On the other hand, the highest ductility of 35% among all the materials was reached in the case of the most CoCrFeNiMn15Al5 alloy which was also the softest one.

Tab. 5 *Mechanical properties of the prepared MA+SPS alloys*

alloy	HV 1	CYS [MPa]	CS [MPa]	ductility [%]
CoCrFeNiMn15Al5	493 ± 3	1458 ± 114	2326 ± 58	35
CoCrFeNiMn10Al10	550 ± 3	1786 ± 38	2314 ± 80	20
CoCrFeNiMn5Al15	668 ± 4	2135 ± 21	2496 ± 21	15

4 Conclusion

The HEAs belong undoubtedly to modern materials, which properties are strongly related to the chosen preparation method and their conditions. In this work, the CoCrFeNiMn15Al5, CoCrFeNiMn10Al10 and CoCrFeNiMn5Al15 alloys were prepared by a combination of MA and compacted via SPS. This combination resulted in ultrafine-grained microstructure composed, in the case of CoCrFeNiMn15Al5 alloy, of disordered solid solutions having FCC and BCC crystallographic lattice. As the content of Al increased, the phase composition changed increasing the amount of newly formed solid solution with PC lattice at the expense of FCC solid solution reducing its content in the CoCrFeNiMn5Al15 alloy down to 36%. The newly formed solid solution with PC lattice was matched with the XRD reference card for the AlNi phase and which content reached up to 39% in the case of CoCrFeNiMn5Al15 alloy. Furthermore, it was shown that the SPS compaction reduced the internal porosity of the formerly prepared powder alloys in some cases by almost 1%. The partial substitution of Mn by Al in the $\text{CoCrFeNiMn}_X\text{Al}_{20-X}$ (X=5, 10, 15) alloy affected the mechanical properties increasing the hardness, CYS and UCS of the alloys reaching its maxima of 668 ± 4 HV1, CYS 2135 MPa and UCS 2496 MPa for the CoCrFeNiMn5Al15 alloy.

Acknowledgement

This research was financially supported by Czech Science Foundation (grant No. 21-11313S).

References

[1] PRUSA, F.; SENKOVA, A.; VOJTECH, D.; CAPEK, J.; BERNATIKOVA, A., High Entropy Alloys Prepared by Combination of Mechanical Alloying and Spark Plasma Sintering. *Manufacturing Technology Journal* 2016, *16* (6), 1350-1354

[2] YANG, G.; XIE, Y.; ZHAO, S.; REN, Y.; WANG, C., Methods and Mechanism of Powder Mixing for Selective Laser Melting. *Manufacturing Technology Journal* 2022, *22* (1), 102-110

[3] VONAVKOVA, I.; VOJTECH, D.; PALOUSEK, D., Characterization of β-Ti alloy prepared by SLM method. *Manufacturing Technology Journal* 2020, *20* (5), 690-696

[4] MICHALCOVA, A.; VOJTECH, D.; KUBATIK, T. F.; NOVAK, P.; DVORAK, P., Structural Description of Powder Metallurgy Prepared Materials. *Manufacturing Technology Journal* 2014, *14* (3), 359-362

[5] KNAISLOVA, A.; KUCERA, D.; MICHALCOVA, A.; MAREK, I.; CYGAN, S.; JAWORSKA, L., Microstructure of AlCrFeSi Alloys Prepared by High-Pressure Spark Plasma Sintering. *Manufacturing Technology Journal* 2018, *18* (5), 753-757

[6] KUCERA, V.; VOJTECH, D., AA 7075 Ultrafine-Grained Alloy Prepared by Mechanical Alloying and Spark Plasma Sintering. *Manufacturing Technology Journal* 2017, *17* (4), 493-498

[7] MAREK, I.; VOJTECH, D.; MICHALCOVA, A.; KUBATIK, T. F., Preparation and Mechanical Properties of Ultra-High-Strength Nanocrystalline Metals. *Manufacturing Technology Journal* 2015, *15* (4), 596-600

[8] PRUSA, F.; VOJTECH, D.; BERNATIKOVA, A.; DVORSKY, D., Mechanical Alloying: A Way How to Improve Properties of Aluminium Alloys. *Manufacturing Technology Journal* 2015, *15* (6), 1036-1043

[9] PRŮŠA, F.; ŠENKOVÁ, A.; KUČERA, V.; ČAPEK, J.; VOJTĚCH, D., Properties of a high-strength ultrafine-grained CoCrFeNiMn high-entropy alloy prepared by short-term mechanical alloying and spark plasma sintering. *Materials Science and Engineering: A* 2018, *734*, 341-352

[10] JI, W.; FU, Z.; WANG, W.; WANG, H.; ZHANG, J.; WANG, Y.; ZHANG, F., Mechanical alloying synthesis and spark plasma sintering consolidation of CoCrFeNiAl high-entropy alloy. *Journal of Alloys and Compounds* 2014, *589*, 61-66